

# Modelling the Fast-ion RF-Pinch Effect with a Toroidally Localised ICRF Antenna

H. Patten<sup>1</sup>, J. Graves<sup>1</sup>, J. Faustin<sup>1</sup>, S. Lanthaler<sup>1</sup>, D. Van Eester<sup>2</sup>, E. Lerche<sup>2</sup>,  
T. Johnson<sup>3</sup> and JET Contributors\*

*EUROfusion Consortium, JET, Culham Science Centre, Abingdon, OX14 3DB, UK*

<sup>1</sup> *SPC-EPFL, Lausanne, Switzerland*

<sup>2</sup> *Association Euratom-Belgian State, LPP-ERM-KMS, B-1000 Brussels, Belgium*

<sup>3</sup> *Alfvén Laboratory, Association EUROATOM/VR, Sweden*

*E-mail: hamish.patten@epfl.ch*

## Introduction

If we consider the toroidal momentum equation in a tokamak, then ICRF heating has the effect of changing the toroidal momentum such that:

$$p_\varphi = -q\psi + mv_{||}B_\varphi|B| \quad \text{with} \quad \Delta p_\varphi \simeq \frac{RB_\varphi}{B\omega}k_{||}\Delta E \quad (1)$$

Thus, for a trapped particle with bounce tips aligned with the resonant ICRF layer, then the change in momentum directly corresponds to a radial motion across flux surfaces, referred to as a ‘pinch’ towards or away from the magnetic axis[6]. Therefore, +90 (co-current) antenna phasing ( $n_\varphi > 0$ ) pinches inwards as  $k_{||} \simeq n_\varphi/R$ , with  $n_\varphi$  the toroidal mode from the Fourier decomposition of the ICRF antenna. The pinch corresponding to this phasing is important to study as future high-performance JET shots will potentially use +90 phasing. The results presented in this paper were carried out using JET plasma profiles determined from shot number 89199 from the M15-27 ‘ICRH scenarios for DT’ experiments. The data implemented in the simulations here was taken using EFIT data. Within this shot 6MW of on-axis ( $B_0 = 3.4T$ ) ICRF heating was applied using the minority heating scheme on the 3%  $^3He$  concentration. Using this data, the SCENIC [1] package was used to study interactions of ICRF heating with fast  $^3He$  particles. Within this work the phasing remains at +90 applied to the minority  $^3He$  species, with each simulation run for a total of 4.5 times the slowing down time on the electrons for convergence.

## Antenna Model

In order to toroidally localise the wave in LEMan, the total electric field will be the summation of the different toroidal wave numbers, the contribution of each wave weighted according to the antenna current spectrum given by:

\*See the Appendix of F. Romanelli et al., Proceedings of the 25th IAEA Fusion Energy Conference 2014, Saint Petersburg, Russia.

$$J_{n_\varphi} = \sum_k j_k^{(n_\varphi)} \frac{\sin(\frac{n_\varphi}{R} W_k)}{\frac{n_\varphi}{R} W_k} \exp\left(-\frac{n_\varphi d}{R}\right) \quad \text{with} \quad j_k^{n_\varphi} = j_{0k} \exp\left(i \frac{n_\varphi}{R} z_k + i \varphi_k\right) \quad (2)$$

Where  $W_k$  is the half width of the antenna strap,  $z_k$  is the strap location and  $\varphi_k$  is the phasing of the antenna. Note that the exponential term includes the effect of the plasma damping on the wave for the outer antenna distance  $d$ .

Therefore LEMan calculates the electric field for each toroidal mode number and the Monte-Carlo ICRF operator implemented in VENUS-LEVIS ensures a coherent reconstruction of the wave according to equation 2. Furthermore, the antenna that is implemented in LEMan is constructed independantly in  $s, \theta$  and  $\varphi$ :

$$J_{ant} = \sigma_s(s) \sigma_\theta(\theta) \sum_n \sigma_n e^{in\varphi} \vec{e}_{ant} \quad (3)$$

Where this box function representation is constructed in the same way for  $s$  and  $\theta$ :

$$\sigma_\alpha(\alpha) = f_B \left( \frac{\alpha - \alpha_1}{\alpha_2 - \alpha_1} \right) (1 - \chi_\alpha^2)^2 \quad (4)$$

For  $\alpha = s, \theta$  and  $f_B$  the box function, and  $\chi_\alpha$  is a polynomial function. The number of toroidal modes included in the simulation has been shown to influence the ICRF behaviour [2], thus for the work carried out here 9 modes of  $n_\varphi \in [8, 16]$  were implemented, each mode chosen according to the magnitude of the mode contribution  $\sigma_n$ .

Evidence of the RF-pinch effect is provided by the population of different orbit types in the plasma, as with a higher inward pinch the trapped resonant particles tend to be driven more towards the passing limit [3]. Thus three different exotic particle orbit types are defined here: potato orbits are trapped particles that circle the magnetic axis, and Low Field Side (LFS) and High Field Side (HFS) cherry orbits, which are co and counter-current passing particles (resp.) which do not circle the magnetic axis. In order to classify the orbits, a simple consideration of the background magnetic equilibrium and the constants of motion of a particle suffices to allow a categorisation of the exotic orbits [4], [5]. Despite the small percentage concentration of these types of orbits, they can have a large influence on the fast-ion current, where for on-axis heating with 3%  $^3He$  the LFS cherry orbits contribute roughly 20% of the fast-ion current. Thus reflecting the importance of the particles close to the trapped-passing boundary.

### $^3He$ Concentration

In actual JET experiments, there is always uncertainty in the percentage concentration of the minority species contained within the plasma. Applying the toroidally localised antenna a concentration scan was performed over 1, 3 and 5%  $^3He$ . The results indicate that minority ICRF heating produces larger fast ion tail temperatures when using lower percentage  $^3He$  concentrations, as expected. Furthermore, both the fast ion pressure and current were found to be considerably larger for lower concentrations. Consequently, the influence on the RF-pinch

was shown by the difference between the number of counter-passing and trapped particles, the populations of which were [14.7%, 51.7%] for 1%, and [20.6%, 44.8%] for 5%  $^3\text{He}$ .

Whereas, the co-passing population remained at  $\sim 34\%$ . As the average ICRF-kick increases for smaller concentrations of the minority species, the particles are pushed closer towards the trapped-passing boundary, forming more exotic orbit types such as the large current driving LFS cherry orbits, shown in figure 1.

### Resonance Position

Throughout the duration of, or inbetween shots, both the resonance layer and magnetic axis can move, therefore it is also important to evaluate the differences between LFS, HFS and central heating on the RF-pinch, in conjunction with a toroidally localised antenna model. A scan over  $B_{\text{res}} \in [3.2, 3.3, 3.4, 3.5, 3.6]$  was carried out, which indicates, as is well established in the ICRF community, that central heating is most beneficial for producing larger fast-ion current and pressure, shown in figure 2.

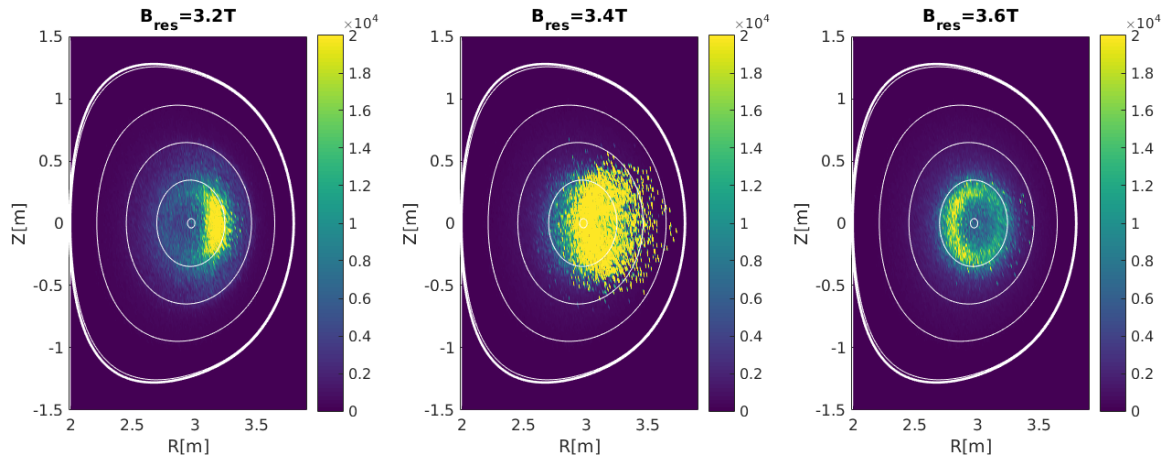


Figure 2: Pressure plots indicating the influence of changing the location of the resonant layer on both the pressure and orbit types

In order to understand the strength of the RF-pinch for the resonant layer position, it is important to note the different mechanisms that produce each orbit, such as HFS heating tends to produce larger amounts of HFS cherry and potato orbits and less LFS cherry orbits than LFS heating, reflected in figure 2, indicating peaked pressure values where the fast-ions tend to be localised, which was also shown in different JET experiments [7].

The results found in figure 3 indicate that the RF-pinch is weakest on  $B_{\text{res}} = 3.2\text{T}$ , as resonance does not occur at the bounce tips, thus the change in toroidal momentum provides a large

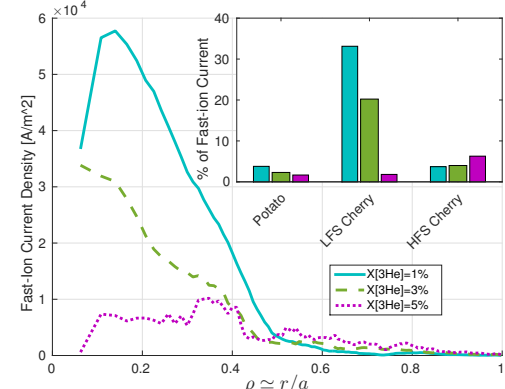


Figure 1: Influence of  $^3\text{He}$  on the Current Density and Exotic Orbit Types

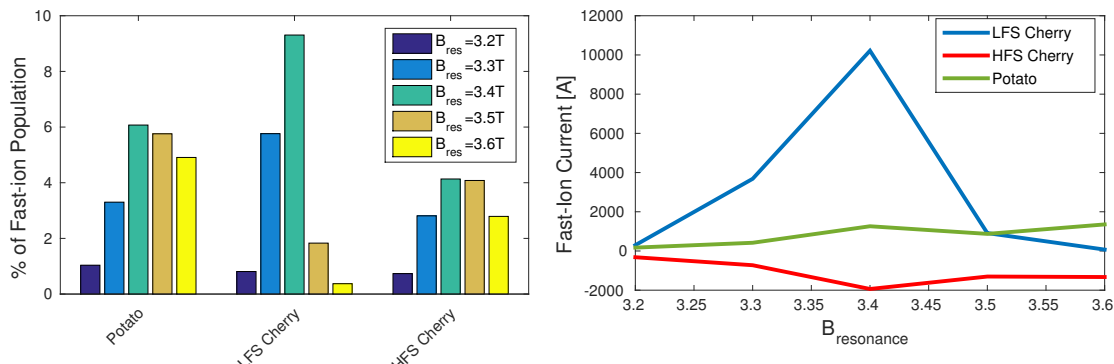


Figure 3: left: Influence of the Resonance Layer on Orbit types, right: the Associated Currents

$\Delta v_{||}$  as well as  $\Delta \psi$ , therefore the radial pinch is less effective. On the other hand,  $B_{res} = 3.6T$  has same fraction of HFS cherry orbit types as for  $B_{res} = 3.3T$  but a larger mean energy, driving larger currents in the counter-direction. Furthermore, HFS heating easily produces large fractions of potato orbits as the trapped banana orbits that are aligned with the resonant layer tend to rapidly increase in energy, thus the banana width increases, to such an extent that the trapped particle then circles the magnetic axis. Additionally, it can be seen that in order to produce large fractions of highly energetic LFS cherry type particle orbits, on-axis heating is required, where the particle remains in the resonance layer and is continuously accelerated until balancing with the loss of energy from collisions with the background.

## Conclusion

The SCENIC package implements a fourier decomposition of the JET ICRF antenna in the toroidal direction. By inclusion of multiple toroidal modes, the RF-pinch effect was explored by exploiting the capability of studying Finite Orbit Width effects with the code. Once the simulations converge it was then possible to categorise the different orbit types of the particles, providing insight into the RF-pinch for varying the  $^3He$  concentration and the position of the resonance layer.

## References

- [1] M. Jucker, et al., Comput. Phys. Commun. **182**, 912–925 (2011)
- [2] R. J. Dumont, AIP Conf. Proc. **1187**, 97 (2009)
- [3] Mantsinen, M.J., 2000, Nuc. Fus. **40**, 10
- [4] J. Hedin, et al., Nuc. Fus. **42**, 527–540 (2002)
- [5] L. G. Eriksson, F. Porcelli, Plasma Phys. Con. Fus. **43**, R145-R182 (2011)
- [6] L. G. Eriksson, et al, Phys. Rev. Lets. **81**, 6 (1998)
- [7] Mantsinen, M.J., 2002, Phys. Rev. Let. **89**, 11

This work has been carried out within the framework of the EUROfusion Consortium and has received funding from the Euratom research and training programme 2014-2018 under grant agreement No 633053. The views and opinions expressed herein do not necessarily reflect those of the European Commission.